

# Behavior of PGS/apatite foam scaffolds during incubation in SBF, PBS, Ringer's solution, artificial saliva, and distilled water

## Badanie inkubacyjne pianek PGS/hydroksyapatyt w SBF, PBS, płynie Ringera, sztucznej ślinie i wodzie destylowanej

Paweł J. Piszko<sup>1,A–E</sup>, Dagmara Słota<sup>2,A,B,D</sup>, Agnieszka Sobczak-Kupiec<sup>2,E,F</sup>, Agnieszka Tomala<sup>2,A,B</sup>, Karina Niziołek<sup>2,A,B</sup>, Wioletta Florkiewicz<sup>2,A</sup>, Konrad Szustakiewicz<sup>1,E,F</sup>

<sup>1</sup> Department of Polymer Engineering and Technology, Faculty of Chemistry, Wrocław University of Science and Technology, Poland

<sup>2</sup> Department of Materials Science, Faculty of Materials Science and Physics, Cracow University of Technology, Poland

A – research concept and design; B – collection and/or assembly of data; C – data analysis and interpretation;

D – writing the article; E – critical revision of the article; F – final approval of the article

Polymers in Medicine, ISSN 0370-0747 (print), ISSN 2451-2699 (online)

Polim Med. 2024;54(2):91–104

### Address for correspondence

Paweł J. Piszko

E-mail: pawel.piszko@pwr.edu.pl

### Funding sources

The “Multifunctional biologically active composites for applications in bone regenerative medicine” project is carried out within the TEAM-NET program of the Foundation for Polish Science financed by the European Union under the European Regional Development Fund (POIR.04.04.00-00-16D7/18).

### Conflict of interest

None declared

Received on December 15, 2023

Reviewed on November 20, 2024

Accepted on November 26, 2024

Published online on December 3, 2024

### Cite as

Piszko PJ, Słota D, Sobczak-Kupiec A, et al. Behavior of PGS/apatite foam scaffolds during incubation in SBF, PBS, Ringer's solution, artificial saliva, and distilled water. *Polim Med.* 2024;54(2):91–104. doi:10.17219/pim/196496

### DOI

10.17219/pim/196496

### Copyright

Copyright by Author(s)

This is an article distributed under the terms of the Creative Commons Attribution 3.0 Unported (CC BY 3.0) (<https://creativecommons.org/licenses/by/3.0/>)

## Abstract

**Background.** Poly(glycerol sebacate) is a polymeric material with potential biomedical application in the field of tissue engineering. In order to act as a biodegradable scaffold, its incubation study is vital to simulate its behavior.

**Objectives.** This study explores the degradation of porous poly(glycerol sebacate)/hydroxyapatite scaffolds subjected to incubation in various physiological solutions.

**Materials and methods.** The research involved monitoring pH and conductivity values over a 14-day period, as well as analyzing the swelling capacity and mass alterations of the scaffolds.

**Results.** In simulated body fluid (SBF) and phosphate-buffered saline (PBS), the pH levels remained relatively stable, whereas Ringer's solution caused a pH decrease. Conversely, artificial saliva demonstrated an increase in pH, and distilled water caused a slight decrease. The conductivity values remained stable in SBF and Ringer's solution, slightly decreased in PBS, increased in artificial saliva, and significantly increased in distilled water. The swelling capacity of the scaffolds varied depending on the solution used, with the lowest equilibrium swelling observed in SBF and PBS. The effect of the presence of ceramics on this parameter was also observed. The mass changes of the scaffolds indicated deposition of particles or salts from the incubation solutions, and subsequent rinsing in distilled water led to a decrease in mass. Scanning electron microscopy (SEM) imaging and elemental analysis confirmed the presence of crystallized salts on the scaffold surfaces after incubation in SBF. Surface roughness measurements revealed changes in roughness depending on the solution, with deposition of additional layers in SBF and degradation in artificial saliva.

**Conclusions.** In summary, the scaffolds exhibited biodegradation in physiological solutions, with variations in pH, conductivity, swelling capacity, mass changes, and surface morphology depending on the specific solution and scaffold composition.

**Key words:** hydroxyapatite, incubation, poly(glycerol sebacate), scaffolds

## Streszczenie

**Wprowadzenie.** Poli(sebacynian gliceryny) to materiał polimerowy o potencjalnym zastosowaniu biomedycznym w dziedzinie inżynierii tkankowej. Aby efektywnie pełnić rolę biodegradowalnego rusztowania komórkowego, niezbędne jest przeprowadzenie badania inkubacyjnego w celu symulacji jego zachowania.

**Cel pracy.** Prezentowane badanie przedstawia zachowanie pianek z poli(sebacynianu gliceryny) oraz hydroksyapatytu podczas inkubacji w różnych roztworach fizjologicznych.

**Materiał i metody.** Badania obejmowały monitorowanie wartości pH i przewodności przez okres 14 dni, a także analizę pęcznienia i zmian masy materiałów.

**Wyniki.** W buforze SBF (ang. simulated body fluid) oraz PBS (ang. phosphate-buffered saline) wartość pH pozostawała na stałym poziomie, podczas gdy w płynie Ringera wartość pH ulegała obniżeniu. Podczas inkubacji w sztucznej ślinie wartości pH wrosły, a w wodzie destylowanej ulegały niewielkiemu obniżeniu. Wartości przewodności pozostawały stabilne w SBF i płynie Ringera. Uległy natomiast niewielkiemu spadkowi w PBS, wzrosły w sztucznej ślinie, a znacznie wzrosły w wodzie destylowanej. Pęcznienie pianek na bazie PGS zależało od użytego roztworu. Najniższe wartości pęcznienia równowagowego zaobserwowano w SBF i PBS. Zmiany masy rusztowań wskazywały na osadzanie się cząstek lub soli z roztworów inkubacyjnych. Przepłukanie materiałów wodą destylowaną powodowało obniżenie masy. Obrazowanie techniką skaningowej mikroskopii elektronowej (SEM) oraz analiza elementarna potwierdziły obecność soli wykrystalizowanych na powierzchniach materiałów po inkubacji w SBF. Pomiar chropowatości wykazał zmiany w wartościach współczynnika Sa w zależności od rodzaju wykorzystanego roztworu. W SBF dochodziło do depozycji dodatkowych warstw apatytowych oraz do zwiększonej degradacji w sztucznej ślinie.

**Wnioski.** Rusztowania wykazywały biodegradację w roztworach fizjologicznych. Różnice w przebiegu inkubacji były ilustrowane pomiarami wartości pH, przewodności, zdolności do pęcznienia, zmianie mas oraz morfologii powierzchni. Różnice wynikały z wykorzystanego roztworu oraz składu pianki.

**Słowa kluczowe:** hydroksyapatyt, inkubacja, poli(sebacynian gliceryny), scaffoldy

## Introduction

Poly(glycerol sebacate) (PGS) is an emerging biodegradable polyester for biomedical application, foremost in tissue engineering.<sup>1–4</sup> This polymeric material is considered biodegradable,<sup>5,6</sup> which is a desired trait for modern biomedical application. However, a biomaterial can behave diversely in various physiological fluids. In this study, PGS was combined with bioactive hydroxyapatite (HAp) in order to obtain porous scaffolds for bone tissue regeneration. This ceramics was selected considering its impressive properties in terms of its impact on osseointegration processes. Hydroxyapatite is widely applied in dentistry as well as orthopedics for its similarity in chemical composition to the inorganic phase of bone.<sup>7–9</sup> For this reason, as well as because of its osteoconductive properties, HAp is used in tissue engineering, with both in vitro and in vivo applications widely reported in the literature.<sup>10</sup> A material exhibiting osteoconductivity ensures the appropriate environment for the ingrowth of bone-forming elements from the surrounding area. Furthermore, by stimulating osteoblasts to proliferate, the growth of new apatite layers occurs.<sup>11,12</sup> Therefore, PGS is a great addition to biomaterials for bone regeneration, especially polymers, which often display significantly lower mechanical strength.<sup>13,14</sup>

In order to simulate the behavior of biomaterials in living organisms, different types of artificial biological fluids are used, of which the most common are simulated body fluid (SBF), artificial saliva, Ringer's fluid (which corresponds to the composition of extracellular fluid), or phosphate-buffered saline (PBS), whose composition corresponds to body fluids.<sup>15–17</sup> Different pH values as well

as the composition of various artificial biological fluids affect the behavior of biomaterials in their presence, and in the case of in vitro tests, they can quickly provide the first information.<sup>18,19</sup> Such incubation studies are particularly important in the context of materials that are assumed to degrade in the body environment. Detailed potentiometric as well as conductometric monitoring helps to determine whether, during the process of degradation of the material into finer elements, there is precipitation and/or release of other components that could negatively affect the cellular balance. Strong acidification, i.e., a spike in pH values to highly alkaline, is a cause for concern, as under such conditions, cells in the area of the implant are unable to proliferate.<sup>20,21</sup> Therefore, in vitro studies are advisable before proceeding to cellular or in vivo studies on animal models.

As the physico-chemical and mechanical properties as well as cytocompatibility with L929 fibroblast cells of the very same materials was reported previously,<sup>22</sup> this study puts an emphasis on the behavior of the PGS and PGS/HAp scaffold materials during incubation. It is crucial to investigate the behavior of the biomaterial in various conditions and incubation fluids in order to consider further clinical application. Graphical scheme of the study is presented in Fig. 1.

## Materials and methods

All of the chemical compounds utilized for synthesis of HAp and obtaining buffers were obtained from Chempur (Piekary Śląskie, Poland), except ammonia solution, which was obtained from Stanlab (Lublin, Poland).

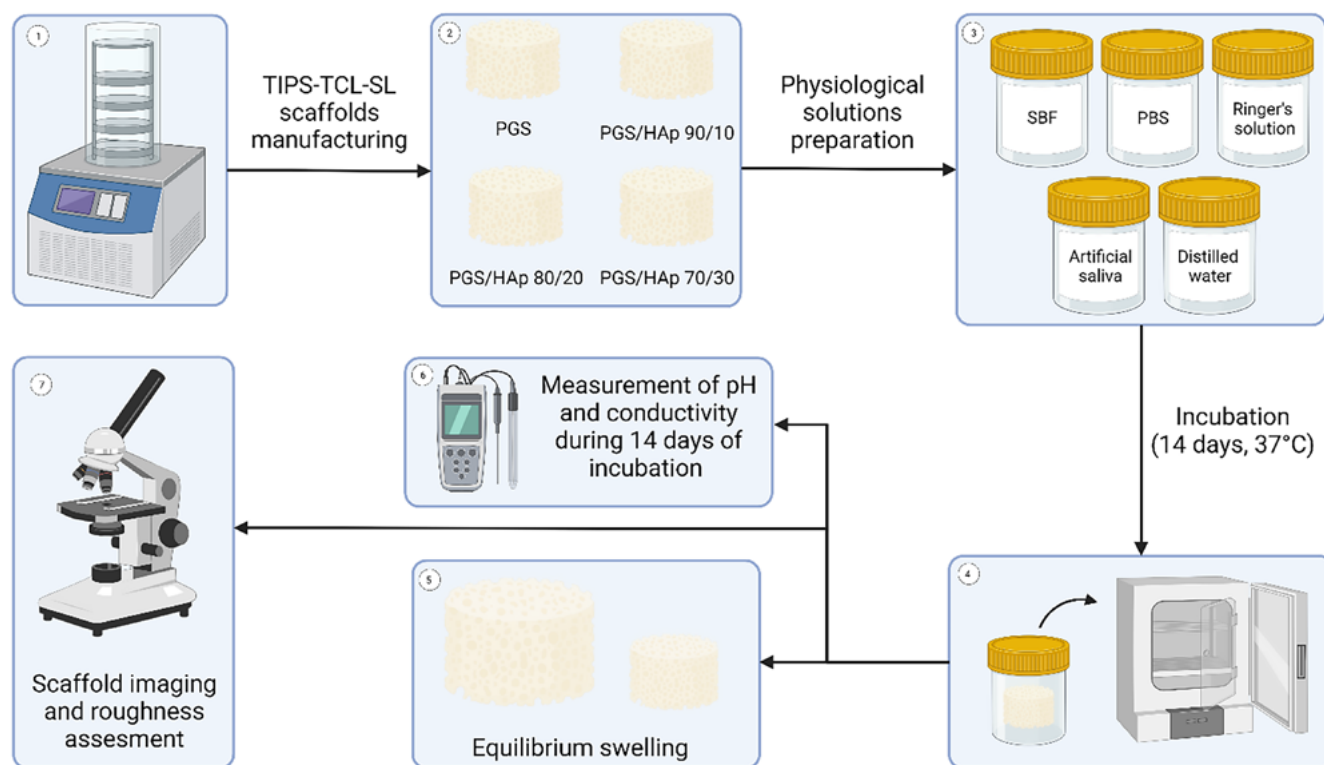


Fig. 1. Graphical scheme of the conducted study, created with BioRender.com

## Synthesis of HAp

The synthesis process followed a previously reported wet precipitation method protocol.<sup>23,24</sup> First, 3.63 g of  $\text{Na}_2\text{HPO}_4$  was dissolved in 80 mL of distilled water. The solution was transferred to the 3-necked, round-bottomed flask equipped with condenser and a thermocouple. Subsequently an additional 520 mL of water was added to dilute the solution. To achieve a pH of 11, a few drops of 25% ammonia solution were carefully added. After boiling the water, a solution of  $\text{Ca}(\text{CH}_3\text{COO})_2$  (created by dissolving 4.51 g of salt in 200 mL of water) was added dropwise with rate of 1 drop/s. After the solution was added, the reaction mixture was cooled to the ambient temperature and transferred to the beaker for sedimentation in the course of 24 h. The precipitate was subsequently washed with water until it reached a neutral pH. After centrifuging, the supernatant was decanted and obtained HAp was submitted to freeze-drying ( $-50^\circ\text{C}$ ,  $p < 10$  Pa) after subsequent freezing ( $-15^\circ\text{C}$ ).

## pPGS prepolymer synthesis and TIPS-TCL-SL scaffold manufacturing

The synthesis of poly(glycerol sebacate) prepolymer (pPGS) followed a previously established procedure by the authors.<sup>22,25</sup> Briefly, sebacic acid and glycerol were combined in an equimolar ratio with glycerol in  $130^\circ\text{C}$ . Reaction was allowed to proceed for 24 h and was halted by reducing the temperature to  $25^\circ\text{C}$ . Porous PGS scaffolds

containing 0, 10, 20, and 30 wt% of HAp were manufactured using thermally induced phase separation followed by thermal cross-linking and salt leaching (TIPS-TCL-SL) technique described previously.<sup>22,23</sup> In brief, pPGS was dissolved in 1,4-dioxane at a concentration of 20 wt% and the corresponding amount of HAp was added to the mixture (with respect to the prepolymer mass) and stirred for 24 h. Solution was poured onto the porogen (400–500  $\mu\text{m}$  NaCl particles) in a multi-well plates and frozen overnight. Afterwards, the specimens were freeze-dried and cured at  $130^\circ\text{C}$  for 7 days. After cross-linking, the porogen was leached out with water and samples were dried before subjecting for further experiments.

The authors had previously conducted physicochemical and structural characterization of the prepolymer<sup>22,23,25</sup> which included identification of characteristic structural bands on Fourier-transform infrared spectroscopy (FT-IR) spectrum, structural characterization with nuclear magnetic resonance (MRI) technique and contact angle measurement. Furthermore, the porous scaffolds manufactured in the same conditions were also characterized with respect to their thermal and mechanical properties.<sup>22</sup>

## Buffer preparation and scaffold incubation

The scaffolds underwent a 14-day incubation period in 5 different physiological solutions: SBF, PBS, Ringer's solution, artificial saliva, and distilled water. A detailed

**Table 1.** Composition of buffers utilized for the study

Solution	Ingredient	Quantity
PBS	NaCl	8.00 g/L
	KCl	0.20 g/L
	Na <sub>2</sub> HPO <sub>4</sub>	1.15 g/L
	KH <sub>2</sub> PO <sub>4</sub>	0.20 g/L
SBF	NaCl	8.04 g/L
	NaHCO <sub>3</sub>	0.36 g/L
	KCl	0.23 g/L
	K <sub>2</sub> HPO <sub>4</sub> ·3H <sub>2</sub> O	0.23 g/L
	MgCl <sub>2</sub> ·6H <sub>2</sub> O	0.31 g/L
	1M HCl	40 mL
	CaCl <sub>2</sub>	0.29 g/L
	Na <sub>2</sub> SO <sub>4</sub>	0.07 g/L
	Tris	6.12 g/L
	1M HCl (for adjusting pH)	0–5 mL
Ringer's solution	NaCl	8.60 g/L
	KCl	0.30 g/L
	CaCl <sub>2</sub> ·2H <sub>2</sub> O	0.48 g/L
Artificial saliva	NaCl	0.40 g/L
	KCl	0.40 g/L
	CaCl <sub>2</sub> ·2H <sub>2</sub> O	0.80 g/L
	Na <sub>2</sub> HPO <sub>4</sub> ·H <sub>2</sub> O	0.78 g/L
	Na <sub>2</sub> S·7H <sub>2</sub> O	0.01 g/L
	urea	1.00 g/L

PBS – phosphate-buffered saline; SBF – simulated body fluid.

breakdown of the composition of the utilized buffers can be found in Table 1. Solutions were obtained by dissolving the appropriate ingredients in distilled water except for the PBS solution, which was prepared by dissolving in water a ready-made commercial product in the form of tablet (Oxoid; Thermo Fisher Scientific, Waltham, USA). The SBF solution was prepared in the sequence presented in the Table 1 in 36.5°C. After all ingredients were dissolved, 1M HCl was added until pH was in the range of 7.5–8.0. The rest of the solutions were prepared in the room temperature. Four scaffolds of each type were placed in separate sterile 100 mL containers and poured over with 75 mL of each buffer. The incubation was performed in ST 5 SMART incubator (POL-EKO, Wodzisław Śląski, Poland) in 37°C for 14 days.

### Buffer preparation and scaffold incubation

Throughout the incubation period, the solutions containing the scaffolds were regularly analyzed for pH and conductivity to investigate interactions between the samples and the incubation fluids. Conductivity and pH were assessed using a CX-701 pH-meter (Elmetron, Zabrze,

Poland). These assessments were conducted at specific time intervals, namely, on the 1<sup>st</sup>, 3<sup>rd</sup>, 7<sup>th</sup>, 9<sup>th</sup>, and 14<sup>th</sup> day of the incubation process.

### Equilibrium swelling

The swelling capacity of the tested scaffolds was assessed in all 5 incubation fluids over a 14-day period, with measurements taken at specific time intervals: 15 min, 30 min, 1 h, 2 h, 4 h, 1 day, 2 days, 7 days, 9 days, and 14 days. Samples with an initial mass ranging from 0.14 g to 0.22 g were placed in sterile 100 mL containers and submerged with 75 mL of the corresponding buffer solution. The swelling ratio ( $S_w$ ) was calculated using Equation 1,<sup>24,26,27</sup> where  $W_t$  is the mass of swollen sample after given time and  $W_0$  is the initial mass of the scaffold.

$$S_w = \frac{W_t - W_0}{W_0} \times 100\% \quad (1)$$

The swelling kinetics of the scaffolds was investigated using Voigt-based viscoelastic model using Equation 2,<sup>28,29</sup> where  $S_t$  is swelling ratio at given time ( $t$ ),  $S_e$  is equilibrium swelling and  $\tau$  is a swelling rate parameter (time required to reach 0.63 of maximum swelling value).<sup>30,31</sup>

$$S_t = S_e \times \left(1 - e^{-\frac{t}{\tau}}\right) \quad (2)$$

The exponential fitting was performed in Origin software v. 2021b (OriginLab Corporation, Northampton, USA). The  $R^2$  Pearson's correlation parameter was higher or equal to 0.92 within each fitting.

### Optical imaging, 3D reconstruction and surface roughness measurement

Surface of the scaffolds were imaged using VHX Series Digital Microscope (Keyence, Osaka, Japan). Images were captured in 4k mode, providing a resolution of 4,000 × 3,000 pixels with additional depth of focus analysis. The CMOS VHZ-700 sensor (Keyence) enabled roughness analysis and the creation of 3D reconstructions of the scaffold surfaces. Scanning electron microscopy (SEM) microphotographs and local elemental analysis measured with energy dispersive spectroscopy (EDS) were registered using SEM Jeol 5510LV system (Jeol, Tokyo, Japan). Measurement parameters included threshold angle of 30° and voltage of 10 kV. The SEM microphotographs were registered with ×500 magnification. Before imaging the samples were spray-coated with gold using Cressington 108 sputter coater (Cressington Scientific Instruments, Watford, UK).

## Results

Structural, physico-chemical and biological properties of porous PGS-based materials was reported by the authors previously.<sup>22,23</sup> Therefore, this article explores divergent

area which is stability, swelling, mass loss, and imaging during in vitro incubation in 5 different physiological solutions. Furthermore, the parameters of HAp synthesized and utilized in the presented study, including surface specific area, crystallinity and imaging, were published previously.<sup>22,32</sup>

## Evolution of pH and conductivity during incubation

During an incubation of scaffolds in the physiological liquids the pH (Fig. 2,3), conductivity values were registered after 1, 3, 7, 9, and 14 days. The reference pH values of the solutions were 7.76 for SBF, 7.27 for PBS, 6.31 for Ringer's solution, 5.07 for artificial saliva, and 6.28 for distilled water. During the process, the pH values remained approximately constant for SBF and PBS. In the Ringer's solution, the pH values lowered after 14 days to 4.90 for PGS, 5.56 for PGS/HAp 90/10, 5.10 for PGS/HAp 80/20, and 5.58 for PGS/HAp 70/30. The decrease was the biggest for PGS and PGS/HAp 80/20 samples. The reverse effect was observed for artificial saliva. The pH values of the solutions increased over the incubation time up to 7.70 for PGS, 7.90 for PGS/HAp 90/10, 8.10 for PGS/HAp 80/20, and 8.70 for PGS/HAp 70/30.

Values of conductivity change with the concentration of the ions during incubation in the environment of solutions imitating physiological conditions.<sup>33</sup> Measured values for the reference solutions were 143.5 mS for SBF, 140.6 mS for PBS, 137.8 mS for Ringer's solution,

29.8 mS for artificial saliva, and 41.2 mS for distilled water. The conductivity remained approximately constant for SBF and Ringer's solution. In PBS, the measurements were also constant. However, they were slightly lower the buffer's reference value. In artificial saliva, a slight increase in measured property was noted (from ~30 mS to ~50 mS for all materials). The highest increase was observed in distilled water (even by 400% for PGS/HAp 80/20).

## Equilibrium swelling

The swelling curves for all evaluated scaffolds were fitted using Equation 2 and presented on Fig. 4. The corresponding values of  $S_e$  and  $\tau$  were juxtaposed in Table 2,3. Swelling analysis was performed for all solutions utilized previously. Based on the evolution of pH and conductivity over time, physiological solutions can be divided into groups: 1) those in which neither pH nor conductivity changed statistically significant over time (G1: SBF and PBS); 2) those in which pH level dropped down during incubation while conductivity was not affected (G2: Ringer's solution); and 3) solution in which both conductivity and pH values changed over the course of 14 days (G3: artificial saliva and distilled water). This division is beneficial for analyzing the swelling capacity of the scaffolds.

In G1, the material with lowest equilibrium swelling was PGS/HAp 70/30 with  $S_e$  of 166.7% in SBF and 236.7% in PBS. It is worth mentioning that in SBF, except for PGS/HAp 70/30 sample, all other materials possessed

**Table 2.** Values of equilibrium swelling for the evaluated scaffolds in SBF, PBS, Ringer's solution, artificial saliva, and distilled water

Solution	Se [%]			
	PGS	PGS/HAp 90/10	PGS/HAp 80/20	PGS/HAp 70/30
SBF	488.7 ±3.7	441.0 ±8.0	646.9 ±9.6	166.7 ±4.7
PBS	335.3 ±14.1	465.5 ±15.9	390.4 ±4.7	236.7 ±7.9
Ringer's solution	211.1 ±6.5	160.2 ±7.1	61.5 ±0.9	43.4 ±0.9
Artificial saliva	536.2 ±19.3	319.6 ±15.9	562.7 ±3.5	530.1 ±10.6
Distilled water	253.7 ±8.4	452.1 ±7.8	436.2 ±6.0	351.9 ±7.3

PBS – phosphate-buffered saline; SBF – simulated body fluid; PGS – poly(glycerol sebacate); HAp – hydroxyapatite.

**Table 3.** Values of  $\tau$  rate parameter for the evaluated scaffolds in SBF, PBS, Ringer's solution, artificial saliva, and distilled water

Solution	$\tau$ [min]			
	PGS	PGS/HAp 90/10	PGS/HAp 80/20	PGS/HAp 70/30
SBF	0.05 ±0.01	0.03 ±0.01	0.03 ±0.01	1.46 ±0.32
PBS	0.94 ±0.38	0.92 ±0.23	0.53 ±0.05	1.17 ±0.24
Ringer's solution	0.66 ±0.23	0.99 ±0.33	0.26 ±0.06	0.73 ±0.27
Artificial saliva	0.63 ±0.21	3.20 ±0.72	2.91 ±0.07	3.39 ±0.25
Distilled water	1.17 ±0.23	0.65 ±0.08	1.98 ±0.13	0.57 ±0.09

PBS – phosphate-buffered saline; SBF – simulated body fluid; PGS – poly(glycerol sebacate); HAp – hydroxyapatite.

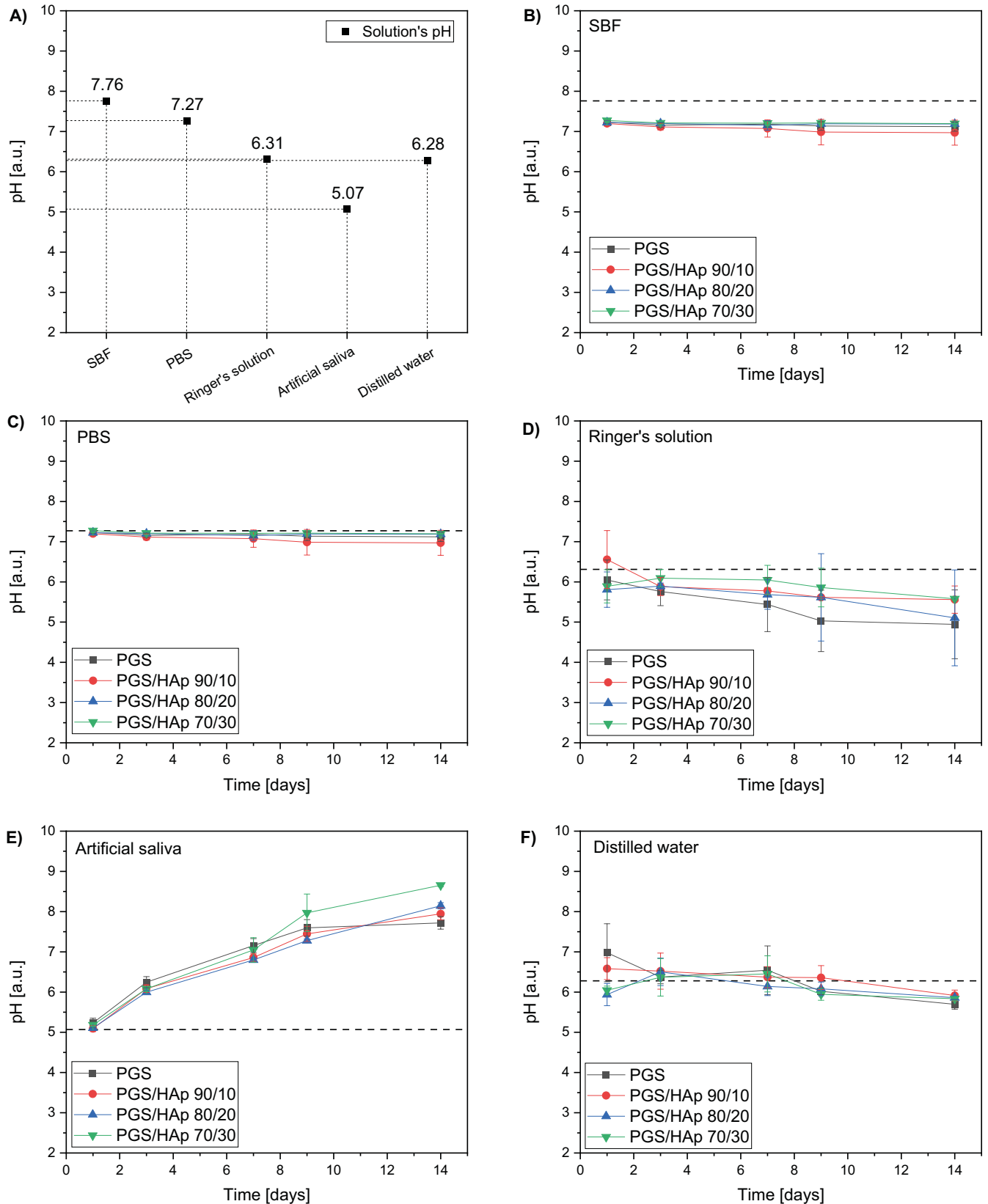


Fig. 2. The pH values of the reference solutions used for incubation of the scaffolds (A) as well its values during 14 days of incubation in simulated body fluid (SBF) (B), phosphate buffered saline (PBS) (C), Ringer's solution (D), artificial saliva (E), and distilled water (F)

the highest  $\tau$  for all measured samples and therefore their swelling was the swiftest. In Ringer's solution (G3) the  $S_e$  swelling was the lowest among all solutions and gradually

lowered with the concentration of HAp (from 211% for PGS down to 43% for PGS/HAp 70/30). The highest  $\tau$  values (except for PGS) were observed in artificial saliva, indicating

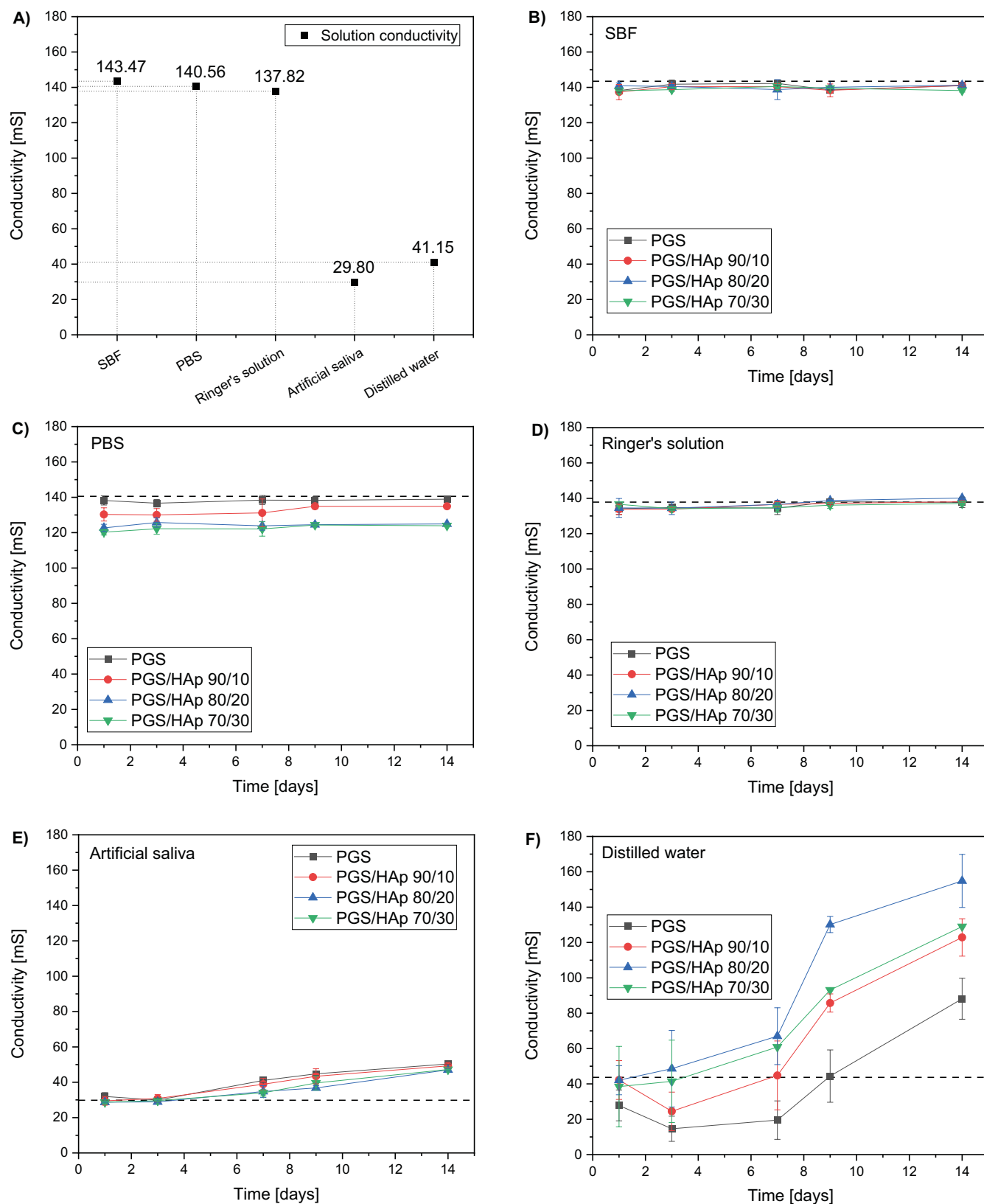


Fig. 3. Conductivity values of the reference solutions used for incubation of the scaffolds (A) as well its values during 14 days of incubation in simulated body fluid (SBF) (B), phosphate buffered saline (PBS) (C), Ringer's solution (D), artificial saliva (E), and distilled water (F).

the highest time required to achieve full swelling capacity (3.20 for PGS/HAp 90/10, 2.91 for PGS/HAp 80/20 and 3.39 for PGS/HAp 70/30). In  $H_2O$ , PGS exhibited lowest

$S_e$  (211%) and PGS/HAp 90/10 the highest (452%). In G3 no direct correlations between pH, conductivity and  $S_e$  is present.

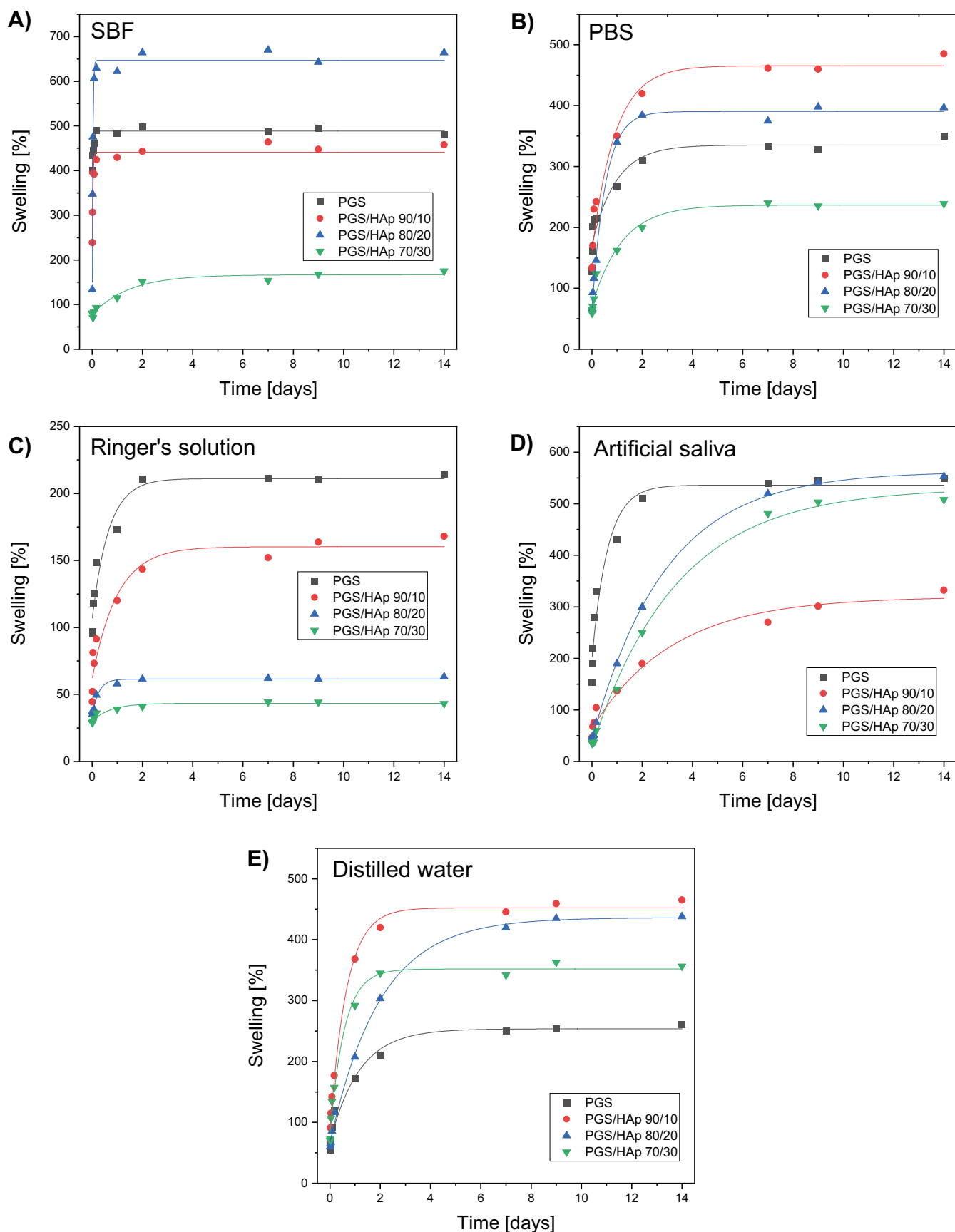


Fig. 4. Swelling of the evaluated scaffolds over 14 days in simulated body fluid (SBF) (A), phosphate buffered saline (PBS) (B), Ringer's solution (C), artificial saliva (D), and distilled water (E).

## Scaffolds' imaging and roughness assessment

The change of scaffolds mass after the incubation is presented in Fig. 5. Samples were weighted directly after drying from incubation solutions (Fig. 5A) and after subsequent rinsing overnight in distilled water (Fig. 5B). For all scaffolds incubated in SBF, PBS and Ringer's solution,

**Table 4.** Weight and atomic % of C, O, Na, Mg, P, Cl, K, and Ca elements based on EDS analysis for the evaluated PGS/HAp 70/20 scaffold incubated in SBF. Presented results concern the points on the SEM images designated as 1 and 2

Sample	PGS/HAp 80/20 in SBF	
Point	1	2
C [at%]	45,061	46,317
C [wt%]	25,250	24,363
O [at%]	5,407	8,768
O [wt%]	4,036	6,144
Na [at%]	20,637	2,023
Na [wt%]	22,135	2,037
Mg [at%]	0,094	0,278
Mg [wt%]	0,106	0,296
P [at%]	0,488	1,898
P [wt%]	0,705	2,575
Cl [at%]	27,288	37,577
Cl [wt%]	45,134	58,343
K [at%]	0,196	0,375
K [wt%]	0,358	0,641
Ca [at%]	0,729	2,655
Ca [wt%]	1,364	4,661

PBS – phosphate-buffered saline; SBF – simulated body fluid; PGS – poly(glycerol sebacate); HAp – hydroxyapatite; SEM – scanning electron microscopy; EDS – energy dispersive spectroscopy.

the change of mass was positive, weighted after drying straight from the incubation solutions.

After subsequent rinsing of the samples in water, the mass decreased in comparison to samples dried directly after incubation in all specimens and solution (Fig. 5B). The change of mass was the most significant in distilled water and dropped to –15% for polymer scaffold.

Moreover, the SEM imaging and EDS measurement revealed that for sample incubated in SBF, crystallized domains of salts present in the buffer composition were observed (Fig. 6). The accurate areas of EDS measurements are indicated as red marks on the SEM image. The detailed elemental composition is presented in Table 4. Most importantly, the majority of abundance consists of Na and Cl elements not present in the initial sample before incubation. The EDS measurement and SEM imaging performed on reference

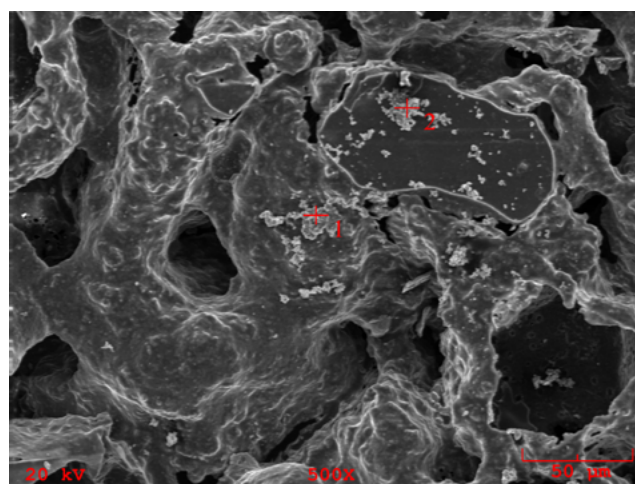


**Fig. 6.** Scanning electron microscopy (SEM) microphotographs of the PGS/HAp 80/20 scaffold after 14 days of incubation in simulated body fluid (SBF). The positions where energy dispersive spectroscopy (EDS) measurements took place are marked with red marks

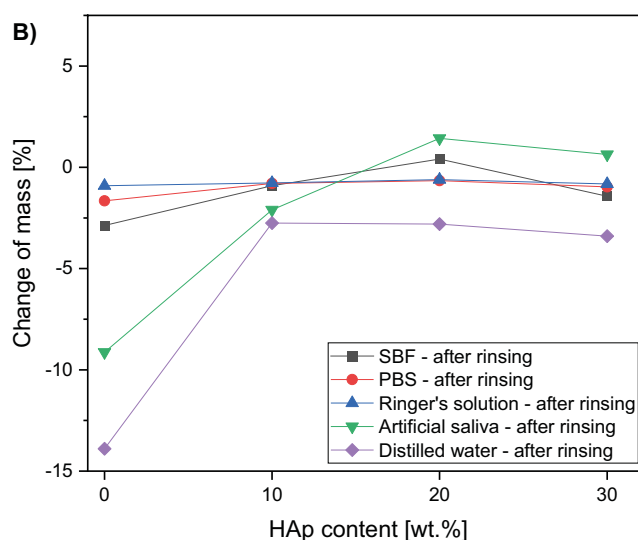
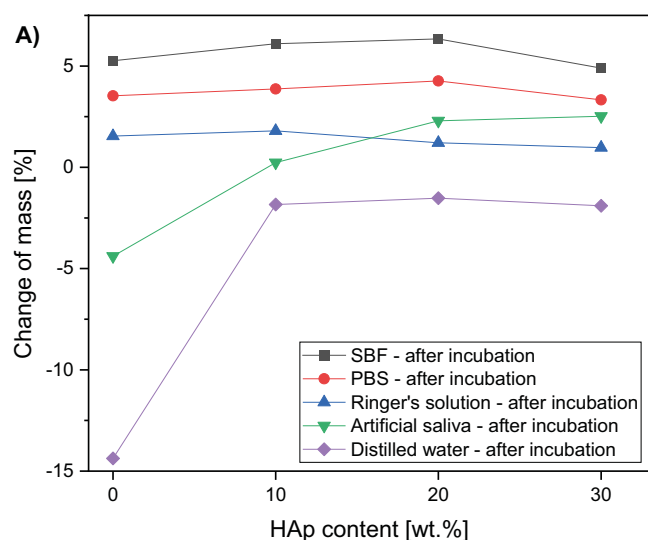


**Fig. 5.** Change in mass of the reference and composite scaffolds after 14 days incubation in simulated body fluid (SBF), phosphate buffered saline (PBS), Ringer's solution, artificial saliva, and distilled water for specimens dried straight after incubation (A) and samples dried followed by rinsing in distilled water in order to remove crystallized impurities (B)

**Table 5.** Surface roughness of the reference and composite scaffolds before and after 2 week of incubation in SBF, PBS, Ringer's solution, artificial saliva, and distilled water

Incubation medium	Sa [ $\mu\text{m}$ ]			
	PGS	PGS/HAp 90/10	PGS/HAp 80/20	PGS/HAp 70/30
Sample before incubation	132.2	116.6	89.0	80.6
SBF	127.7	101.2	74.0	63.6
PBS	113.8	97.7	58.8	42.5
Ringer's solution	127.9	77.5	63.7	18.9
Artificial saliva	177.2	122.3	105.2	63.9
Distilled water	123.4	112.8	91.2	76.2

PBS – phosphate-buffered saline; SBF – simulated body fluid; PGS – poly(glycerol sebacate); HAp – hydroxyapatite; Sa – arithmetical mean height of the area.

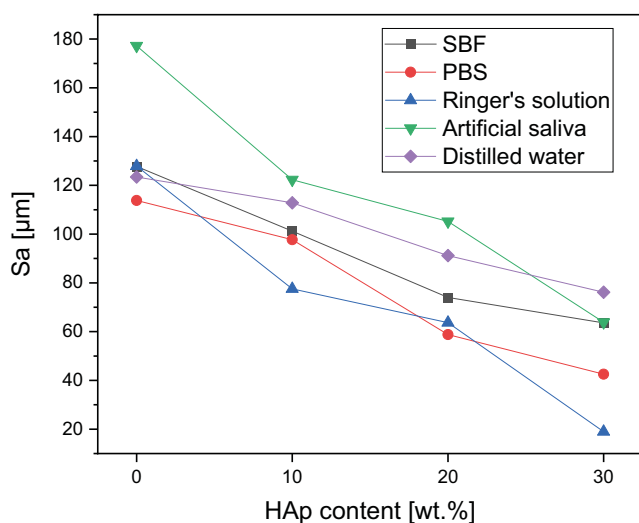


**Fig. 7.** Surface roughness of the reference and composite scaffolds after 2 week of incubation in simulated body fluid (SBF), phosphate buffered saline (PBS), Ringer's solution, artificial saliva, and distilled water. Roughness data was measured as an arithmetical mean height of the area (Sa) and showcased in the function of filler content

PGS and PGS/HAp scaffolds before incubation showcased the morphology and confirmed presence of apatite filler.<sup>22</sup>

The morphological changes are depicted by the evolution of the surface roughness measurement basing on 3D reconstructions from the optical microscope (VHX Series Digital Microscope; Keyence) (Fig. 7). For the reference samples before the incubation, a decrease in roughness can be observed as the amount of apatite filler increases: 132.2  $\mu\text{m}$  for PGS, 116.6  $\mu\text{m}$  for PGS/HAp 90/10, 89.0  $\mu\text{m}$  for PGS/HAp 80/20, and 80.6  $\mu\text{m}$  for PGS/HAp 90/30. This downward trend with the increasing amount of HAp persisted for all utilized solutions. Surface roughness before and after incubation is also presented in the Table 5.

Surface all of the samples before and after 14 days of incubation in SBF, PBS, Ringer's solution, and distilled water were registered in the form of 2D images, presented in Fig. 8,9. The morphology of the top layer of the scaffolds was visualized using a 3D reconstruction of microscopic images captured on optical microscope (VHX Series

Digital Microscope; Keyence). Exemplary photographs of reference samples and samples incubated in SBF and artificial saliva are presented in Fig. 10.

## Discussion

In artificial saliva, the greatest increased in pH values were observed among all evaluated buffers. One of the explanations of this effect may lay in the initial slightly acidic pH of the reference solution (5.08) – it may catalyze the degradation process of the scaffolds. Additionally, the ions released during the incubation might have influenced further changes in the pH values. Moreover, during incubation, partial leaching of HAp from the matrix might have occurred.<sup>34</sup> Despite its poor solubility, the solution containing HAp might have gained additional alkaline character.<sup>35</sup> In distilled water, a slight lowering in a pH from the reference value was noted. Changes in the pH value indicate interactions occurring at the fluid–material interface as well as the fact that the foams interact with the medium. In cases of inert (neutral) material, the pH value would remain at a constant level.

Regarding values of conductivity, such steep rise in values in distilled water might be correlated with low ionic force of water, which is disturbed by sudden introduction of new electrostatically charged beings to the solution.<sup>36</sup> Furthermore, in all showcased experiments, using distilled water eliminated the interference of other ions in the solution with evaluated scaffold.

The swelling ability of the material is related to the penetration of the liquid medium into its interior into the free spaces of the polymer chains.<sup>37</sup> In the case of composites, ceramic grains occupy these spaces; hence, a decrease in sorption capacity is observed as the proportion of the ceramic phase increases. However, even a low swelling capacity is a satisfactory result, as such a material can be used as a carrier for an active substance, from which the substance (e.g., a drug, protein or antibiotic) will be able to be slowly released as the liquid medium penetrates into the material.<sup>38–40</sup>

The changes in surface roughness of the scaffolds might indicate either deposition on new HAp particles or salts

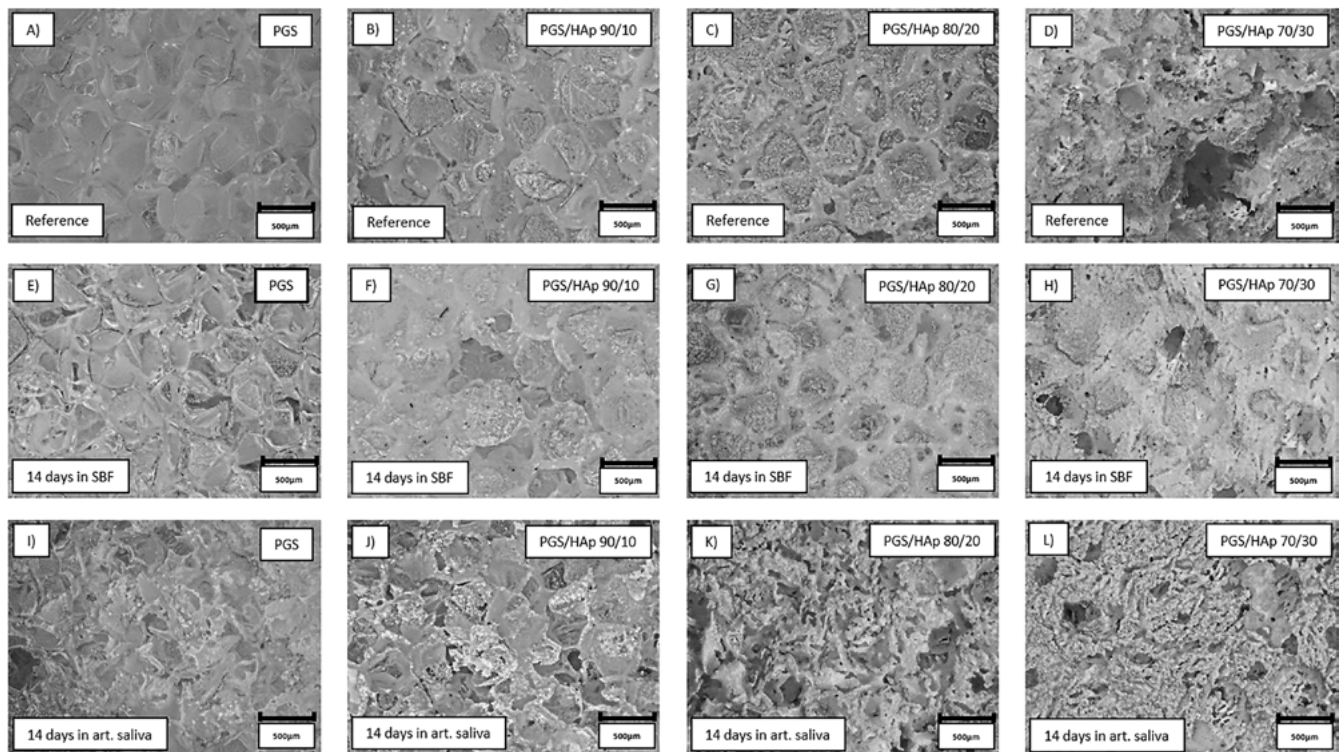


Fig. 8. Optical microscope images depicting surface of reference samples before incubation (A–D) as well as after 14 days of incubation in simulated body fluid (SBF) (E–H) and artificial saliva (I–L). Photographs were taken with  $\times 100$  magnification

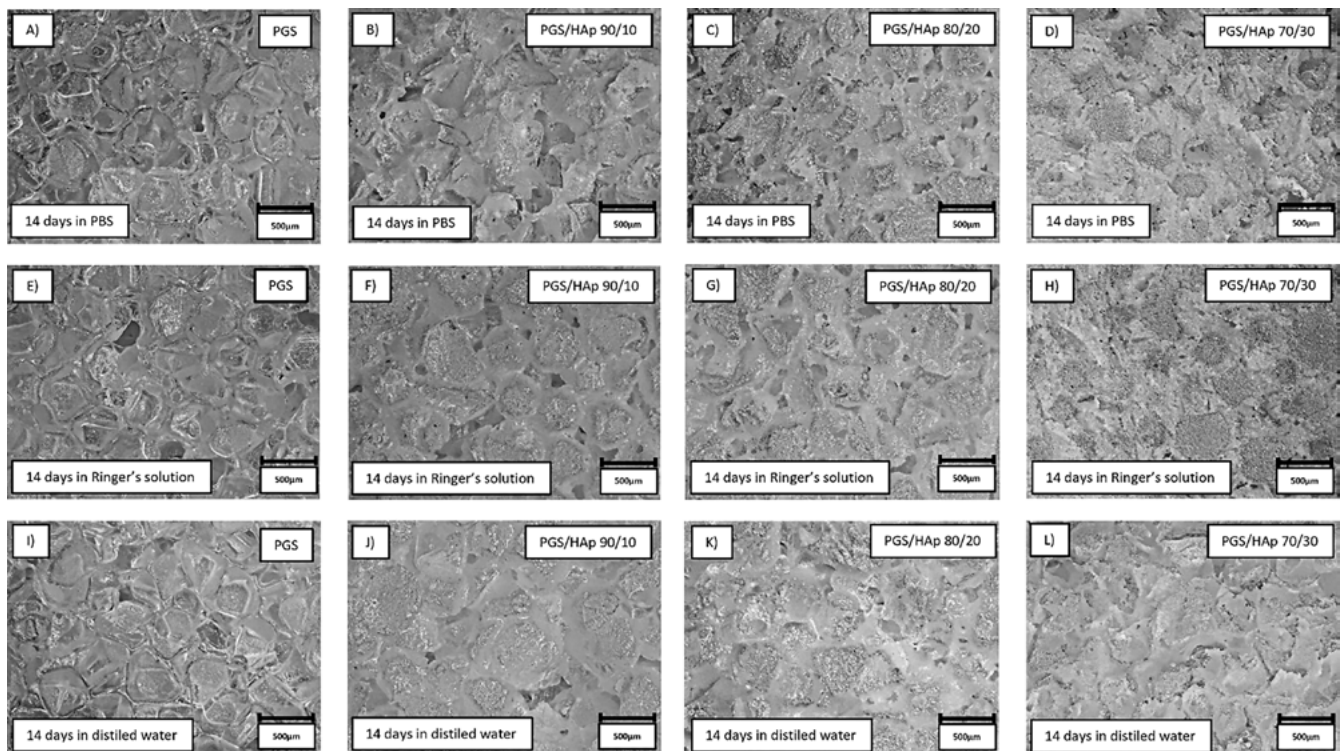


Fig. 9. Optical microscope images depicting surface of samples after 14 days of incubation in phosphate buffered saline (PBS) (A–D), Ringer's solution (E–H) and distilled water (I–L). Photographs were taken with  $\times 100$  magnification

present in the solutions. In case of polymer scaffolds, the HAp is not present and thus the gain in mass is due to the plausible crystallization of the salts present in solutions. This hypothesis was confirmed by decrease in mass

for all samples incubated in distilled water, which does not contain statistically significant concentrations of ions. The increase of the pH value during incubation in artificial saliva was the greatest among all measured solutions,

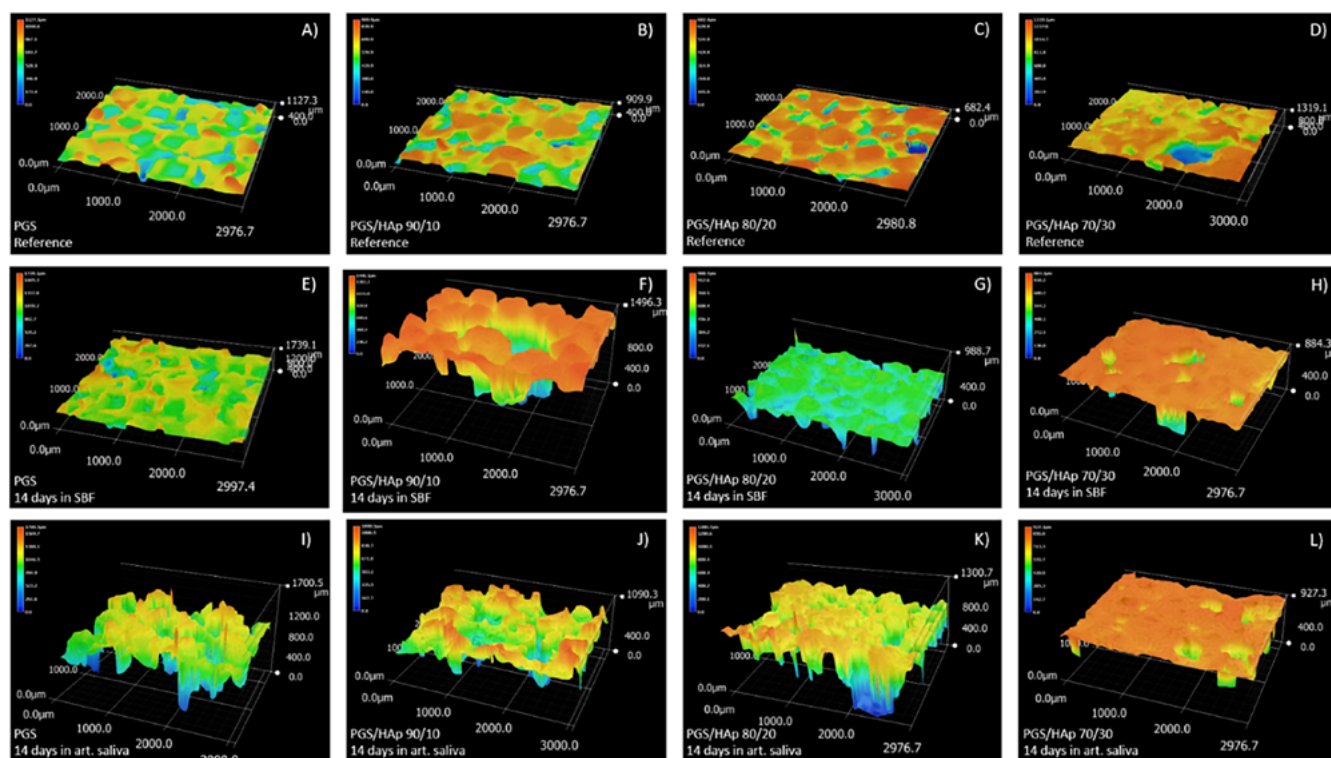


Fig. 10. Three-dimensional reconstructions of the surface of reference samples before incubation (A–D) as well as after 14 days of incubation in simulated body fluid (SBF) (E–H) and artificial saliva (I–L). The topography was obtained using reconstruction mode of optical microscope based on the pictures were taken with  $\times 100$  magnification

which might be an indication of degradation process occurring.<sup>41</sup> This was confirmed by loss in mass for PGS sample (approx.  $-5\%$ ). For specimens containing the apatite filler in artificial saliva, the mass change was positive – again most probably due to the salts present in the solution. The initial conclusion regarding crystallization of salts from incubation solutions was supported with changes in mass after subsequent rinsing in water before drying following incubation. Noticeably, the roughness of samples incubated in the distilled water overlapped with the reference values almost ideally. Moreover, the presented data indicate that the artificial saliva was the only solution for which the roughness was greater than for the reference sample. It might be yet another indication of degradation process occurring in this solution. For all other physiological solutions (SBF, PBS and Ringer's solution), the roughness was lowered in comparison with the reference. Therefore, deposition of additional layers on top of the scaffolds might have occurred. As it is clearly visible after incubation in SBF, deposition of additional layers on the surface was observed, while in saliva, the structure appear more frayed and degraded, except for PGS/HAp 70/30 sample.

## Conclusions

We investigated the initial (14 days) degradation stage of PGS scaffolds, as well as PGS doped with HAp in 5 different liquids – distilled water, SBF, PBS, Ringer's fluid, and artificial

saliva. The results obtained in SBF, PBS, Ringer's solution, and artificial saliva provide a biologically relevant context for potential biomedical applications, as these media simulate the environment of body fluids. Water serves as a reference medium to assess baseline degradation properties. The study showed that scaffold of neat PGS showed the lowest stability, understood as weight loss during degradation ( $-15\%$  after 14 days of incubation), while doped PGS showed significantly higher stability ( $-2\%$  after 14 days of incubation). The effect obtained does not depend significantly on the ceramic content (similar values were obtained for systems containing 10, 20 and 30 wt% of ceramics). The greatest loss of PGS scaffold masses is particularly related to degradation in distilled water and artificial saliva. Electrical conductivity tests carried out during incubation showed no significant differences for samples incubated in SBF, PBS and Ringer's fluid, while in the case of artificial saliva, an increase in conductivity was observed from a level of approx.  $30 \mu\text{S}$  at the start of incubation to more than  $40 \mu\text{S}$  after 14 days of incubation in all samples tested. Incubation conducted in distilled water led to an increase in conductivity from a level of approx.  $30 \mu\text{S}$  to  $80 \mu\text{S}$  for the reference sample and from approx.  $40 \mu\text{S}$  to  $120\text{--}150 \mu\text{S}$  for the composite scaffolds. This effect is related to the degradation of the PGS and the ingress of mineral matter from the composite into solution. The observed degradation is a beneficial process, as it will eventually be combined with the regeneration of autologous tissue, which aligns with the goals of biomedical applications where scaffold resorption supports tissue regeneration.

The conclusions for future research highlight the necessity for further investigation of long-term degradation beyond the initial 14 days, as well as the exploration of the effects of additional ceramic additives and bioactive compounds on scaffold performance. Furthermore, in vivo validations are required to confirm the behavior of the scaffold in physiological conditions and its integration with tissue. A limitation of this study is that it focuses exclusively on in vitro conditions, which may not fully capture the complexities of the in vivo environment.

## ORCID iDs

Paweł J. Piszko  <https://orcid.org/0000-0002-7577-8509>  
 Dagmara Słota  <https://orcid.org/0000-0002-8570-3594>  
 Agnieszka Sobczak-Kupiec  <https://orcid.org/0000-0003-0005-6146>  
 Agnieszka Tomala  <https://orcid.org/0000-0002-2327-3947>  
 Karina Niziołek  <https://orcid.org/0000-0001-7970-3478>  
 Wioletta Florkiewicz  <https://orcid.org/0000-0002-9392-4362>  
 Konrad Szustakiewicz  <https://orcid.org/0000-0002-2855-852X>

## References

- Piszko P, Kryszak B, Piszko A, Szustakiewicz K. Brief review on poly (glycerol sebacate) as an emerging polyester in biomedical application: Structure, properties and modifications. *Polim Med.* 2021;51(1): 43–50. doi:10.17219/pim/139585
- Vogt L, Ruther F, Salehi S, Boccaccini AR. Poly(glycerol sebacate) in biomedical applications: A review of the recent literature. *Adv Healthcare Mater.* 2021;10(9):2002026. doi:10.1002/adhm.202002026
- Rai R, Tallawi M, Grigore A, Boccaccini AR. Synthesis, properties and biomedical applications of poly(glycerol sebacate) (PGS): A review. *Prog Polym Sci.* 2012;37(8):1051–1078. doi:10.1016/j.progpolymsci.2012.02.001
- Loh XJ, Abdul Karim A, Ow C. Poly(glycerol sebacate) biomaterial: Synthesis and biomedical applications. *J Mater Chem B.* 2015; 3(39):7641–7652. doi:10.1039/C5TB01048A
- Pomerantseva I, Krebs N, Hart A, Neville CM, Huang AY, Sundback CA. Degradation behavior of poly(glycerol sebacate). *J Biomed Mater Res A.* 2009;91A(4):1038–1047. doi:10.1002/jbm.a.32327
- Wang Y, Kim YM, Langer R. In vivo degradation characteristics of poly(glycerol sebacate). *J Biomed Mater Res A.* 2003;66A(1):192–197. doi:10.1002/jbm.a.10534
- Wei Y, Chen M, Li M, et al. Aptamer/hydroxyapatite-functionalized titanium substrate promotes implant osseointegration via recruiting mesenchymal stem cells. *ACS Appl Mater Interfaces.* 2022;14(38): 42915–42930. doi:10.1021/acsmi.2c10809
- Kim J, Kang IG, Cheon KH, et al. Stable sol–gel hydroxyapatite coating on zirconia dental implant for improved osseointegration. *J Mater Sci Mater Med.* 2021;32(7):81. doi:10.1007/s10856-021-06550-6
- Szwed-Georgiou A, Płociński P, Kupikowska-Stobba B, et al. Bioactive materials for bone regeneration: Biomolecules and delivery systems. *ACS Biomater Sci Eng.* 2023;9(9):5222–5254. doi:10.1021/acsbio materials.3c00609
- Brogini S, Sartori M, Giavaresi G, et al. Osseointegration of additive manufacturing Ti–6Al–4V and Co–Cr–Mo alloys, with and without surface functionalization with hydroxyapatite and type I collagen. *J Mech Behav Biomed Mater.* 2021;115:104262. doi:10.1016/j.jmbbm. 2020.104262
- Chang BS, Lee CK, Hong KS, et al. Osteoconduction at porous hydroxyapatite with various pore configurations. *Biomaterials.* 2000;21(12): 1291–1298. doi:10.1016/S0142-9612(00)00030-2
- Kumar D, Gittings JP, Turner IG, Bowen CR, Bastida-Hidalgo A, Cartmell SH. Polarization of hydroxyapatite: Influence on osteoblast cell proliferation. *Acta Biomater.* 2010;6(4):1549–1554. doi:10.1016/j.actbio. 2009.11.008
- Ramesh N, Moratti SC, Dias GJ. Hydroxyapatite–polymer biocomposites for bone regeneration: A review of current trends. *J Biomed Mater Res B Appl Biomater.* 2018;106(5):2046–2057. doi:10.1002/jbm.b.33950
- Mahanty A, Shikha D. Changes in the morphology, mechanical strength and biocompatibility of polymer and metal/polymer fabricated hydroxyapatite for orthopaedic implants: A review. *J Polym Eng.* 2022; 42(4):298–322. doi:10.1515/polypeng-2021-0171
- Yilmaz B, Pazarceviren AE, Tezcaner A, Evis Z. Historical development of simulated body fluids used in biomedical applications: A review. *Microchem J.* 2020;155:104713. doi:10.1016/j.microc.2020.104713
- Baino F, Yamaguchi S. The use of simulated body fluid (SBF) for assessing materials bioactivity in the context of tissue engineering: Review and challenges. *Biomimetics.* 2020;5(4):57. doi:10.3390/biomimetics5040057
- Leung VWH, Darvell BW. Artificial salivas for in vitro studies of dental materials. *J Dent.* 1997;25(6):475–484. doi:10.1016/S0300-5712(96) 00068-1
- Schille Ch, Braun M, Wendel HP, et al. Corrosion of experimental magnesium alloys in blood and PBS: A gravimetric and microscopic evaluation. *Mater Sci Eng B.* 2011;176(20):1797–1801. doi:10.1016/j. mseb.2011.04.007
- Pandey AK, Kumar A, Kumar R, Gautam RK, Behera CK. Tribological performance of SS 316L, commercially pure Titanium, and Ti6Al4V in different solutions for biomedical applications. *Mater Today Proc.* 2023;78(Pt 4):A1–A8. doi:10.1016/j.matpr.2023.03.736
- Vlădescu A, Părau A, Pană I, et al. In vitro activity assays of sputtered HAp coatings with SiC addition in various simulated biological fluids. *Coatings.* 2019;9(6):389. doi:10.3390/coatings9060389
- Ruan C, Hu N, Ma Y, et al. The interfacial pH of acidic degradable polymeric biomaterials and its effects on osteoblast behavior. *Sci Rep.* 2017;7(1):6794. doi:10.1038/s41598-017-06354-1
- Piszko P, Kryszak B, Gazińska M, et al. The effect of filler content on mechanical properties and cell response of elastomeric PGS/apatite foam scaffolds. *Ceram Int.* 2023;49(15):25353–25363. doi:10.1016/j. ceramint.2023.05.071
- Piszko P, Włodarczyk M, Zielińska S, et al. PGS/HAp microporous composite scaffold obtained in the TIPS-TCL-SL method: An innovation for bone tissue engineering. *Int J Mol Sci.* 2021;22(16):8587. doi:10.3390/ijms22168587
- Słota D, Florkiewicz W, Pięta K, et al. Preparation, characterization, and biocompatibility assessment of polymer-ceramic composites loaded with *Salvia officinalis* extract. *Materials (Basel).* 2021;14(20):6000. doi:10.3390/ma14206000
- Piszko P, Kryszak B, Szustakiewicz K. Influence of cross-linking time on physico-chemical and mechanical properties of bulk poly(glycerol sebacate). *Acta Bioeng Biomech.* 2022;24(4):85–93. doi:10.37190/ABB- 02208-2023-04
- Zhang X, Jia C, Qiao X, Liu T, Sun K. Porous poly(glycerol sebacate) (PGS) elastomer scaffolds for skin tissue engineering. *Polym Testing.* 2016;54:118–125. doi:10.1016/j.polymertesting.2016.07.006
- Chen QZ, Bismarck A, Hansen U, et al. Characterisation of a soft elastomer poly(glycerol sebacate) designed to match the mechanical properties of myocardial tissue. *Biomaterials.* 2008;29(1):47–57. doi:10.1016 /j.biomaterials.2007.09.010
- Omidian H, Hashemi SA, Sammes PG, Meldrum I. A model for the swelling of superabsorbent polymers. *Polymer (Guildf).* 1998;39(26): 6697–6704. doi:10.1016/S0032-3861(98)00095-0
- Moini N, Kabiri K. Effective parameters in surface cross-linking of acrylic-based water absorbent polymer particles using bisphenol A diethylene glycidyl ether and cycloaliphatic diepoxide. *Iran Polym J.* 2015;24(11):977–987. doi:10.1007/s13726-015-0386-4
- Kabiri K, Omidian H, Hashemi SA, Zohuriaan-Mehr MJ. Synthesis of fast-swelling superabsorbent hydrogels: Effect of crosslinker type and concentration on porosity and absorption rate. *Eur Polym J.* 2003;39(7): 1341–1348. doi:10.1016/S0014-3057(02)00391-9
- Pluta K, Florkiewicz W, Malina D, et al. Measurement methods for the mechanical testing and biocompatibility assessment of polymer-ceramic connective tissue replacements. *Measurement.* 2021; 171:108733. doi:10.1016/j.measurement.2020.108733
- Słota D, Pięta K, Florkiewicz W, et al. Clindamycin-loaded nano-sized calcium phosphates powders as a carrier of active substances. *Nanomaterials.* 2023;13(9):1469. doi:10.3390/nano13091469
- Słota D, Głąb M, Tyliaszczak B, et al. Composites based on hydroxyapatite and whey protein isolate for applications in bone regeneration. *Materials (Basel).* 2021;14(9):2317. doi:10.3390/ma14092317

34. Heimann RB, Graßmann O, Jennissen HP, Zumbirk T. Biomimetic processes during in vitro leaching of plasma-sprayed hydroxyapatite coatings for endoprosthetic applications. *Materialwissenschaft und Werkstofftechnik*. 2001;32(12):913–921. doi:10.1002/1521-4052(200112)32:12<913::AID-MAWE913>3.0.CO;2-H
35. Sobczak-Kupiec A, Pluta K, Drabczyk A, Włóś M, Tyliszczak B. Synthesis and characterization of ceramic–polymer composites containing bioactive synthetic hydroxyapatite for biomedical applications. *Ceram Int*. 2018;44(12):13630–13638. doi:10.1016/j.ceramint.2018.04.199
36. Smedley SI. *The Interpretation of Ionic Conductivity in Liquids*. Boston, USA: Springer US; 1980. doi:10.1007/978-1-4684-3818-5
37. Karadag E, Saraydin D, Çetinkaya S, Güven O. In vitro swelling studies and preliminary biocompatibility evaluation of acrylamide-based hydrogels. *Biomaterials*. 1996;17(1):67–70. doi:10.1016/0142-9612(96)80757-5
38. Pietrzyńska M, Tomczak R, Jezierska K, Voelkel A, Jampilek J. Polymer-ceramic monolithic in-needle extraction (MINE) device: Preparation and examination of drug affinity. *Mater Sci Eng C Mater Biol Appl*. 2016;68:70–77. doi:10.1016/j.msec.2016.05.097
39. Carreño G, Marican A, Vijayakumar S, et al. Sustained release of linezolid from prepared hydrogels with polyvinyl alcohol and aliphatic dicarboxylic acids of variable chain lengths. *Pharmaceutics*. 2020;12(10):982. doi:10.3390/pharmaceutics12100982
40. Słota D, Florkiewicz W, Pięta K, et al. Preparation of PVP and beta-ine biomaterials enriched with hydroxyapatite and its evaluation as a drug carrier for controlled release of clindamycin. *Ceram Int*. 2022;48(23):35467–35473. doi:10.1016/j.ceramint.2022.08.151
41. Woodard LN, Grunlan MA. Hydrolytic degradation and erosion of polyester biomaterials. *ACS Macro Lett*. 2018;7(8):976–982. doi:10.1021/acsmacrolett.8b00424